Supplementary Information (SI) for Journal of Materials Chemistry C.

Supporting Information

FRET-Relayed Magneto-Photoluminescence Driven by Triplet-Pair Dynamics in Organic Films

Haidi Liu, Chenyang Zhao, Xinhuan Xu, Qiong Wang, Wangliang Li, Qingda Chang, Yanqing Hu, Chuang Zhang, Jiannian Yao and Yongli Yan*

Table of Contents

Materials and experimental details

Materials

Rubrene (purity 99%) and DBP (purity 98%) was purchased from Aladdin and used as received. Quartz substrates were cleaned sequentially by ultrasonication in isopropanol, deionized water, ethanol, and acetone for 30 minutes each, followed by oxygen plasma treatment. Rubrene films (~300 nm thick) were fabricated via thermal evaporation under a vacuum of 1×10^{-4} Pa at a deposition rate of 0.4 Å·s^{-1}. DBP-doped rubrene films (~300 nm thick) were prepared through thermal co-evaporation under the same vacuum conditions using a commercial evaporator (Angstrom Engineering). The doping concentration was defined as the ratio of the DBP deposition rate to that of rubrene. The as-deposited amorphous DBP-doped rubrene films were annealed at 150 °C in a nitrogen atmosphere to induce crystallization.

Optical characterizations

Fluorescence, bright-field, and polarized optical microscopy images were acquired using a polarizing microscope (Nikon, Eclipse LV100NPol). UV-vis absorption spectra were recorded using a Hitachi UH4150 spectrophotometer. The photoluminescence quantum yield (PLQY) was measured using photoluminescence spectrometer (FLS980, Edinburgh Instruments). Magneto-optical measurements were carried out on a custom-built setup integrating a closed-cycle cryostat and an electromagnet (Cryostation s50, Montana Instruments). During all measurements, the sample chamber was maintained under vacuum (< 2.0 Torr) to minimize air-induced quenching. Magneto-photoluminescence (MPL) measurements were performed under excitation with a 532 nm CW laser (MDL-PS-532, CNI). Photoluminescence (PL) was collected and directed either to a spectrograph (SpectraPro HRS-300-MS, Teledyne Princeton Instruments) connected to a deep-cooled CCD (PIXIS 265E, Teledyne Princeton Instruments) or to a silicon photodiode (SM1PD1A, Thorlabs) for real-time intensity monitoring. The photodiode output was amplified using a transimpedance amplifier (PDA200C, Thorlabs), and read out with a digital multimeter (DMM6500, Keithley). Time-resolved PL (TRPL) decays were acquired using time-correlated single-photon counting (TCSPC) with picosecond excitation at 530 nm (FWHM ~10 nm) generated from a filtered supercontinuum source (SC-PRO, YSL Photonics). Emission photons was detected using a single-photon counting module (SPCM-AQRH-14, Excelitas) and processed with a time-to-digital converter (quTAG, qutools).

Transient absorption (TA) measurements

TA measurements were performed using a femtosecond TA spectrometer (Helios, Ultrafast Systems) powered by a commercial Ti:sapphire regenerative amplifier (Spitfire ACE, Spectra-Physics), delivering 800 nm pulses at 1 kHz with ~90 fs duration. The pump beam at 400 nm was generated via second-harmonic generation of the fundamental 800 nm output. A white-light continuum probe was produced by focusing a small portion of the 800 nm beam onto a sapphire plate.

Results and discussion

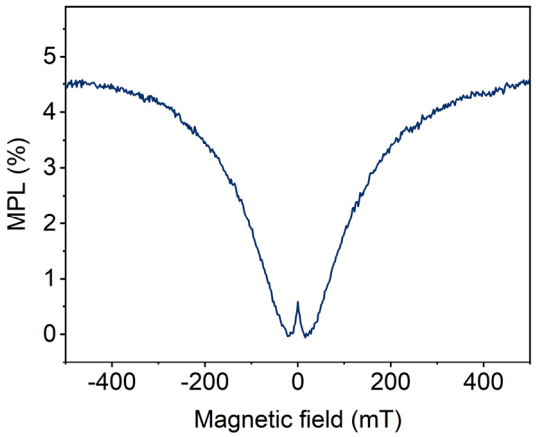

Figure S1. MPL response of a pristine rubrene film.

The pristine rubrene film displays a characteristic “W”-shaped MPL signature, which arises predominantly from magnetic-field-induced spin mixing within spin-correlated triplet-triplet (TT) pairs.

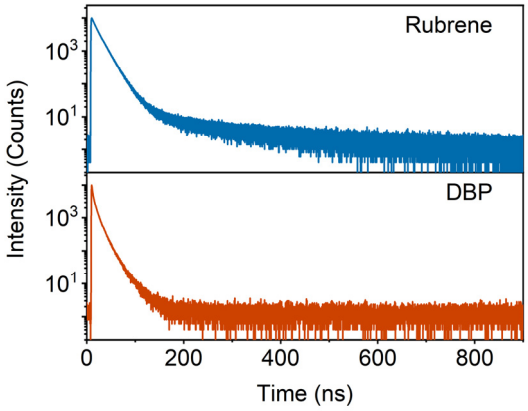

Figure S2. TRPL of rubrene and DBP films.

Rubrene shows a prominent delayed fluorescence component arising from triplet-mediated processes, whereas DBP exhibits a much faster decay that completes within 200 ns and follows an almost single-exponential temporal profile.

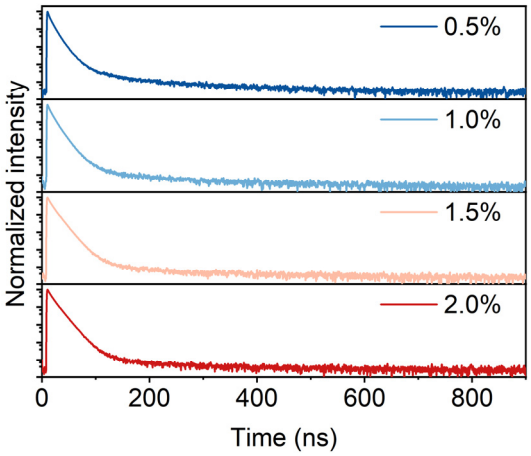

Figure S3. TRPL of DBP-doped rubrene films with varying doping concentrations.

The TRPL dynamics exhibit a clear dependence on DBP doping level. Lower DBP concentrations lead to a stronger delayed-fluorescence contribution. This trend indicates more efficient singlet-fission and an increased population of TT pairs.

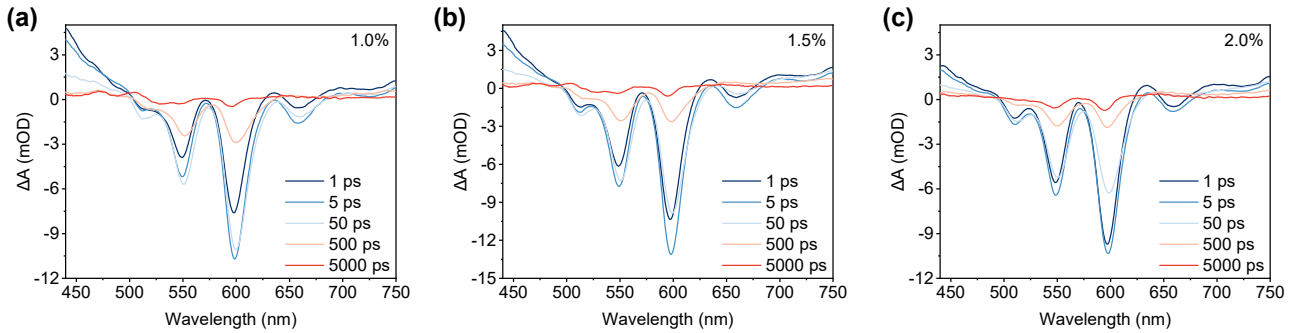

Figure S4. TA spectra of DBP-doped rubrene films with varying doping concentrations.

Compared with the TA spectra of the 0.5%-doped film shown in Fig. 2b, the spectra acquired at other doping levels show nearly identical peak positions, suggesting that the nature of the excited-state species in the DBP-doped rubrene films is largely preserved across the examined doping range.

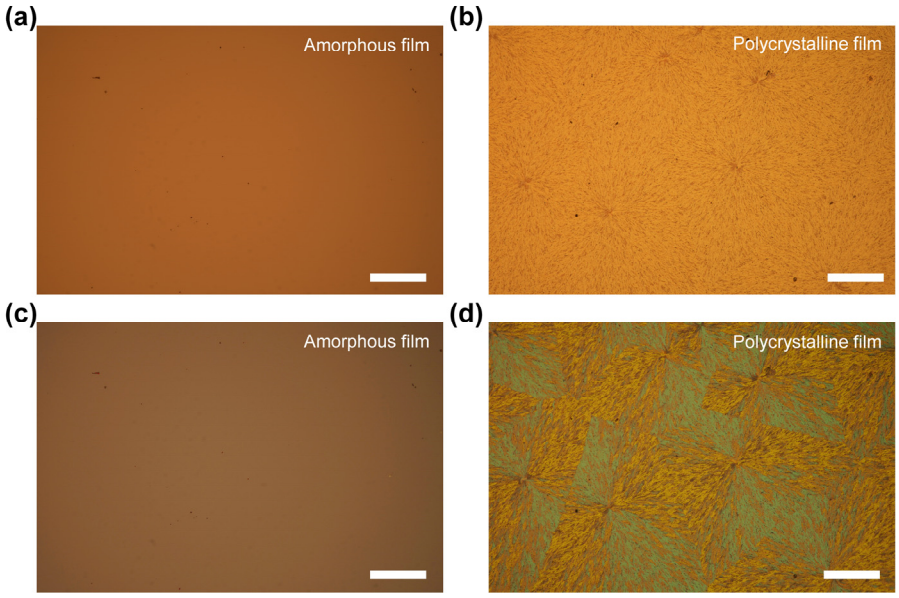

Figure S5. Bright-field (a–b) and polarized optical microscopy (c–d) images of DBP-doped rubrene films before and after crystallization. Scale bars: 100 µm.

Bright-field and polarized optical microscopy images confirm that thermal annealing converts the initially amorphous DBP-doped rubrene films into polycrystalline films with well-defined crystalline domains.

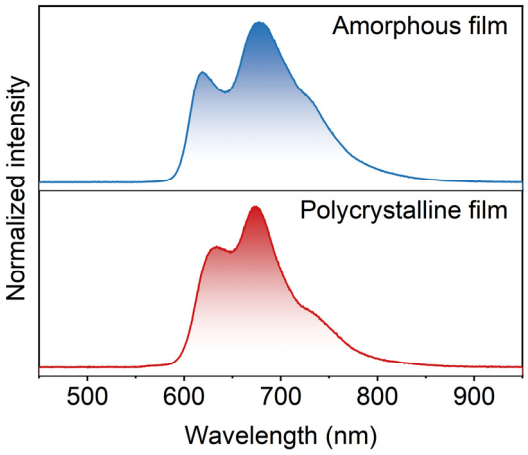

Figure S6. PL spectra of DBP-doped rubrene films before and after crystallization.

After thermal annealing, the PL spectrum exhibits obvious spectral narrowing and enhanced vibronic resolution, reflecting improved molecular packing and a modified local environment around DBP. These spectral changes are consistent with altered host-guest packing arrangement and suggests a modulation of energy transfer process upon crystallization.

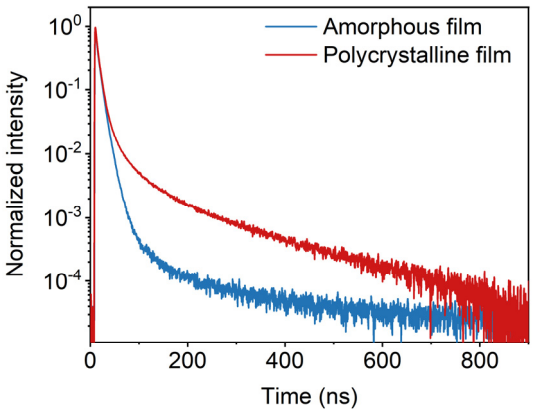

Figure S7. TRPL of DBP-doped rubrene films before and after crystallization.

Thermal annealing markedly enhances the delayed fluorescence, indicating that improved molecular packing in DBP-doped rubrene films facilitates more efficient formation of TT pairs and reinforces spin-correlated excited-state pathways.

Doping concentration	PLQY
0.5%	0.523
1.0%	0.577
1.5%	0.610
2.0%	0.210
0.5%-Cry	0.233

Table S1. Measured absolute PLQY values for different samples. "0.5%-Cry" refers to the sample with 0.5% doping concentration that has undergone crystallization.

The PLQY shows a clear dependence on both DBP doping concentration and crystallization. Specifically, as the DBP concentration increased from 0.5% to 1.5%, the PLQY gradually increases. This behavior is consistent with a reduced contribution from singlet fission and TT-pair formation in rubrene, as a larger fraction of singlet excitons is transferred to DBP via FRET. Upon thermal crystallization, however, the PLQY decreases markedly (from 0.523 to 0.233), which correlates with enhanced intermolecular coupling, increased TT-pair formation, and a strengthened singlet-fission channel in rubrene. At a higher DBP concentration of 2.0%, however, the PLQY drops sharply. This behavior is most likely attributable to concentration-induced quenching arising from excessive DBP loading, which can introduce additional non-radiative decay pathways. These trends are fully consistent with the TRPL and transient absorption results and support the kinetic picture proposed in this work.